Fluid mechanics of nodal flow due to embryonic primary cilia: Electronic Supplementary Material

D. J. Smith, J. R. Blake and E. A. Gaffney

December 20, 2007

1 The volume flow rate due to a conically rotating tilted cilium protruding from a surface

Below we use the resistive force theory of Gray and Hancock (1955) to derive an expression for the average volume flow rate produced by a tilted, conically rotating cilium. We use the formula for the volume flow rate due to a point-force near a cell surface boundary given by Liron (1978), which can be derived from the far-field expression of Blake (1971, 1972).

1.1 Parameterisation of the cilium beat

The slender body or cilium of length L will be described at a time t by $\mathbf{X}(s,t)$, where s is the arc-length, with $0 \leq s \leq L$. If the cilium is taken to be straight, and rotates about the $z = x_3$ axis with semi-cone angle ψ and radian frequency ω then we have the parametric representation:

$$\begin{aligned} X_1 &= s\sin\psi\cos\omega t, \\ X_2 &= -s\sin\psi\sin\omega t, \\ X_3 &= s\cos\psi. \end{aligned} \tag{1}$$

This describes a clockwise rotation viewed from above.

We shall take the $x = x_1$ axis to be the 'left/right' axis of the embryo, with positive x corresponding to the 'left' and the $y = x_2$ axis to be the anterior/posterior axis, with negative y corresponding to the posterior. Hence the net fluid flow will be in the positive x direction and the tilt is in the negative y direction. The plane $z = 0$ represents the cell surface, and $z > 0$ is the extracellular fluid compartment. This is shown on the left of Figure 1.

Applying the posterior tilt with angle θ it is straightforward to show that the parametric representation now becomes:

$$\begin{aligned} X_1 &= s\sin\psi\cos\omega t, \\ X_2 &= -s\sin\psi\sin\omega t\cos\theta - s\cos\psi\sin\theta, \\ X_3 &= -s\sin\psi\sin\omega t\sin\theta + s\cos\psi\cos\theta. \end{aligned} \tag{2}$$

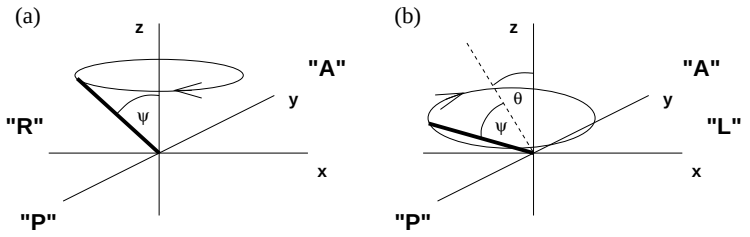

Figure 1: The conical rotation model for an embryonic nodal cilium, with semi-cone angle ψ and posterior tilt θ. Positive x corresponds to the 'left' of the node and negative x to the 'right'; positive y corresponds to the anterior, negative y to the posterior, as indicated. (a) indicates the cilium motion with zero tilt, (b) indicates the cilium motion with non-zero posterior tilt.

The tilted rotation is shown on the right of Figure 1. From the above expression we calculate the partial derivatives $\partial\mathbf{X}/\partial t$ and $\partial\mathbf{X}/\partial s$ for use in the force density expression of Section 1.4.

1.2 Stokes flow equations

We use the mathematical model of Stokes flow, which is appropriate due to the Reynolds number being very much smaller than unity. If the radian frequency speed is estimated to be $2\pi\times 10\,\mathrm{rad/s}$, the cilium length $3\,\mu$m and the viscosity no less than that of water, 0.001 Pa s, then the Reynolds number is no larger than approximately 5×10^{-7}, so Stokes flow is an excellent approximation. The Stokes flow equations are:

$$\begin{aligned} \nabla p &= \mu\nabla^2\mathbf{u}, \\ \nabla\cdot\mathbf{u} &= 0, \end{aligned} \tag{3}$$

where $\mathbf{u}$ is the velocity field, p the pressure and μ the dynamic viscosity.

1.3 Slender body theory

Slender body theory exploits the linearity of the Stokes flow equations (3) in order to describe the fluid flow around a moving body by replacing it with a centreline distribution of point-forces or 'Stokeslets' S_{ij}, weighted by force density $f_j(s,t)$:

$$u_i(\mathbf{x}) = \int_0^L S_{ij}(\mathbf{x},\mathbf{X}(s,t))\,f_j(s,t)\mathrm{d}s. \tag{4}$$

The Stokeslet kernel $S_{ij}(\mathbf{x},\mathbf{X})$ denotes the i-component of the flow velocity at location $\mathbf{x}$ due to a unit point-force in the j-direction located at $\mathbf{X}$. In an infinite fluid this is well-known to be

$$S_{ij}^{\infty} = \frac{1}{8\pi\mu}\left(\frac{\delta_{ij}}{|\mathbf{x}-\mathbf{X}|} + \frac{(x_i-X_i)(x_j-X_j)}{|\mathbf{x}-\mathbf{X}|^3}\right). \tag{5}$$

Cilia protrude from a cell surface on which the no-slip, no-penetration boundary conditions $u_i = 0$ for $i = 1,2,3$ must be satisfied. This is achieved by employing the image system found by Blake (1971), consisting of an equal and opposite image Stokeslet combined with higher order derivatives and the potential flow source dipole solution located at the image point $(X_1, X_2, -X_3)$. This 'singularity combination' allows the representation of fluid flows in the semi-infinite domain $x_3 > 0$, and so we denote it by $S_{ij}^{\infty/2}$. Although the node may also be covered by an additional membrane some distance above the cilia tips, the dominant effect on the flow in the ciliated region is the cell surface boundary. For a recent review of slender body theory for cilia-driven flows and further developments, see Smith et al. (2007).

In this calculation we shall be concerned with the volume flow rate in the x_1 direction due to a point-force in the x_j direction, defined as

$$q_{1j}(X_3) := \int_{x_2=-\infty}^{\infty} \int_{x_3=0}^{\infty} S_{1j}^{\infty/2}(\mathbf{x}, \mathbf{X}) \, \mathrm{d}x_2 \, \mathrm{d}x_3. \tag{6}$$

By conservation of mass q_{1j} is independent of x_1 and X_1, and since $S_{ij}^{\infty/2}$ depends on x_2 and X_2 only through their difference, is also independent of X_2. It is also clear by conservation of mass that the far-field form of q_{1j} is all that is required to compute the flow rate. Blake (1971) showed that for $j = \alpha = 1,2$ the far-field flow due to a unit point-force near a boundary has the 'stresslet' form (see also Blake, 1972):

$$S_{1\alpha}^{\infty/2} \sim \frac{1}{8\pi\mu} \left(\frac{12 X_3 x_1 x_\alpha x_3}{|\mathbf{x}|^5} \right) + O\left(\frac{1}{|\mathbf{x}|^3} \right). \tag{7}$$

This decays with inverse-square of distance, and hence the integral remains finite for large $|\mathbf{x}|$. By symmetry it is clear that in fact $q_{12} = 0$, whereas the double integral of $x_1^2 x_3 / |\mathbf{x}|^5 \sim 2/3$ yields $q_{11} = X_3/(\pi\mu)$ (see also Liron, 1978, Eqn. (3.4)). By contrast, the far-field of $S_{13}^{\infty/2}$ decays with inverse-cube of distance, and hence by taking $|\mathbf{x}|$ to be large we see that the volume flow rate q_{13} is zero.

Hence the volume flow rate at time t due to a force distribution $f_j(s,t)$ for $0 \le s \le L$, with height $X_3(s,t)$ above a no-slip boundary at $z = 0$ is given by

$$\int_0^L \frac{X_3(s,t)}{\pi\mu} f_1(s,t) \, \mathrm{d}s. \tag{8}$$

1.4 Resistive force theory

In order to pursue an analytic expression for the volume flow rate we apply the resistive force theory approximation to slender body theory, as first used by Gray and Hancock (1955). From resistive force theory, the force density is approximated by

$$f_j = C_T \left(\gamma \delta_{jk} - (\gamma - 1) \frac{\partial X_j}{\partial s} \frac{\partial X_k}{\partial s} \right) \frac{\partial X_k}{\partial t}, \tag{9}$$

where we have used the summation convention and δ_{jk} is the Kronecker Delta distribution (Blake, 1972). The parameter C_T is the resistance coefficient for tangential motion,

and γ is the ratio of the normal and tangential resistance coefficients C_N/C_T. Considerable work has been done on improving the values and ratios of these coefficients, see for example the recent work of Gueron and Levit-Gurevich (1999, 2001) who consider a model which combines the efficiency of resistive force theory with the 'non-local' effects in a manner similar to a slender body model. Nevertheless, the precise value of C_N will not affect our conclusions regarding the configuration for optimal advection.

We shall derive the 'leftward' flow in the $x = x_1$ direction, which arises from the integral of $f_1(s,t)$ along the flagellum. Expanding equation (9) for f_1 we have

$$f_1 = C_T \left(\gamma \frac{\partial X_1}{\partial t} - (\gamma - 1) \frac{\partial X_1}{\partial s} \left[\frac{\partial X_1}{\partial s}\frac{\partial X_1}{\partial t} + \frac{\partial X_2}{\partial s}\frac{\partial X_2}{\partial t} + \frac{\partial X_3}{\partial s}\frac{\partial X_3}{\partial t} \right] \right). \tag{10}$$

The terms in equation (10) are given by:

$$\begin{aligned}
\frac{\partial X_1}{\partial t} &= -\omega s \sin\psi \sin\omega t, && (11)\\
\frac{\partial X_1}{\partial s} &= \sin\psi \cos\omega t, && (12)\\
\frac{\partial X_1}{\partial s}\frac{\partial X_1}{\partial t} &= -\omega s \sin^2\psi \cos\omega t \sin\omega t, && (13)\\
\frac{\partial X_2}{\partial s}\frac{\partial X_2}{\partial t} &= \omega s (\sin^2\psi \cos^2\theta \sin\omega t \cos\omega t \\
&\quad + \sin\psi \cos\psi \sin\theta \cos\theta \cos\omega t), && (14)\\
\frac{\partial X_3}{\partial s}\frac{\partial X_3}{\partial t} &= \omega s (\sin^2\psi \sin^2\theta \sin\omega t \cos\omega t \\
&\quad - \sin\psi \cos\psi \sin\theta \cos\theta \cos\omega t). && (15)
\end{aligned}$$

It can be seen immediately that the terms in $\sin\psi\cos\psi\sin\theta\cos\theta\cos\omega t$ in equations (14) and (15) cancel. Using the relation $\sin^2\theta + \cos^2\theta = 1$ we additionally find that the remaining terms in equations (13) to (15) cancel. Recalling that $C_N = \gamma C_T$, we are left with simply

$$f_1 = -C_N \omega s \sin\psi \sin\omega t. \tag{16}$$

1.5 Mean volume flow rate

To calculate the mean volume flow rate Q we integrate (8) over one beat cycle $0 \le t \le 2\pi/\omega$ and divide by the beat cycle duration $T = 2\pi/\omega$:

$$Q = \frac{1}{T}\int_0^T \int_0^L \frac{X_3(s,t)}{\pi\mu} f_1(s,t)\, \mathrm{d}s\, \mathrm{d}t. \tag{17}$$

Using the definition of $X_3(s,t)$ and equation (16), we obtain the simple expression

$$Q = \frac{C_N \omega L^3}{6\pi\mu} \sin^2\psi \sin\theta. \tag{18}$$

This leads to values for the Nonaka et al. (2005) experimental study of

$$Q = (1/8\pi\mu)C_N\omega L^3 \sin\theta \quad \text{for } \psi = 60^o \quad \text{and} \tag{19}$$

$$Q = (1/12\pi\mu)C_N\omega L^3 \sin\theta \quad \text{for } \psi = 45^o. \tag{20}$$

The formula for Q defines a non-negative, non-decreasing function of ψ and θ in the domain $\theta, \psi \geqslant 0$ and $\theta + \psi \leqslant 90^o$. This implies that the maximum lies on the boundary of the domain, i.e. on $\theta + \psi = 90^o$—the configuration reported by Okada et al. (2005). We note that this corresponds to the cilium centreline actually touching $z = 0$ and so cannot occur precisely in the real system, but rather that the value of $\theta + \psi$ will be very close to 90^o.

Returning to the mathematical problem of maximising Q, we substitute $\theta = 90^o - \psi$ and differentiate the resulting expression with respect to ψ. We hence find that the maximum value occurs for semicone angle $\psi = \arctan\sqrt{2} = 54.7^o$ and tilt angle $\theta = 35.3^o$.

References

Blake, J. R. (1971). A note on the image system for a stokeslet in a no slip boundary. *Proc. Camb. Phil. Soc.*, 70:303–310.

Blake, J. R. (1972). A model for the micro-structure in ciliated organisms. *J. Fluid Mech.*, 55:1–23.

Gray, J. and Hancock, G. J. (1955). The propulsion of sea-urchin spermatozoa. *J. Exp. Biol.*, 32(4):802–814.

Gueron, S. and Levit-Gurevich, K. (1999). Energetic considerations of ciliary beating and the advantage of metachronal coordination. *Proc. Natl. Acad. Sci. USA*, 96(22):12240–12245.

Gueron, S. and Levit-Gurevich, K. (2001). A three-dimensional model for ciliary motion based on the internal 9+2 structure. *Proc. R. Soc. Lond. B*, 268:599–607.

Liron, N. (1978). Fluid transport by cilia between parallel plates. *J. Fluid Mech.*, 86(4):705–726.

Nonaka, S., Yoshiba, S., Watanabe, D., Ikeuchi, S., Goto, T., Marshall, W. F., and Hamada, H. (2005). De novo formation of left-right asymmetry by posterior tilt of nodal cilia. *PLoS Biol.*, 3(8):e268.

Okada, Y., Takeda, S., Tanaka, Y., Izpisúa Belmonte, J.-C., and Hirokawa, N. (2005). Mechanism of nodal flow: a conserved symmetry breaking event in left-right axis determination. *Cell*, 121:633–644.

Smith, D. J., Gaffney, E. A., and Blake, J. R. (2007). Discrete cilia modelling with singularity distributions: application to the embryonic node and the airway surface liquid. *Bull. Math. Biol.*, 69(5).